

Covariant separable interaction for the neutron-proton system in 3S_1 - 3D_1 partial-wave state

S. G. Bondarenko^a, V. V. Burov^a, W-Y. Pauchy Hwang^b, E. P. Rogochaya^{a,*}

^a*Bogoliubov Laboratory of Theoretical Physics, Joint Institute for Nuclear Research, Dubna, Russia*

^b*National Taipei University, Taipei 106, Taiwan*

Abstract

Within a covariant Bethe-Salpeter approach a rank-six separable neutron-proton interaction kernel for the triplet coupled 3S_1 - 3D_1 partial-wave state is constructed. Two different methods of a relativistic generalization of initially nonrelativistic form factors parametrizing the kernel are considered. The model parameters are determined by fitting the elastic 3S_1 and 3D_1 phase shifts and the triplet scattering length as well as the asymptotic D/S ratio of the deuteron wave functions and the deuteron binding energy. The D -state probability constraints 4-7% are taken into account. The deuteron magnetic moment is calculated. The half-off-shell properties are further demonstrated by the NoyesKowalski functions. The first test of the constructed kernel is performed by calculating the deuteron electrodisintegration at three different kinematic conditions.

Keywords: phase shifts, separable kernel, Bethe-Salpeter equation, neutron-proton elastic scattering, deuteron

PACS: 11.10.St, 11.80.Et, 13.75.Cs

*Corresponding author. JINR, Joliot-Curie 6, 141980 Dubna, Moscow region, Russia. Tel.: +74962163503; fax: +74962165146

Email addresses: bondarenko@jinr.ru (S. G. Bondarenko), burov@theor.jinr.ru (V. V. Burov), wylwang@phys.ntu.edu.tw (W-Y. Pauchy Hwang), rogoch@theor.jinr.ru (E. P. Rogochaya)

1. Introduction

The deuteron has been an object of intensive investigations as the simplest bound neutron-proton system. Throughout more than 40 years many methods for the description of the deuteron have been elaborated [1]-[17]. The main goal of any approach is the description of the interaction between two nucleons. It is presented either by potentials in the Schrödinger equation or interaction kernels in the Bethe-Salpeter (BS) equation. They are either constructed from the presentation of the interaction as an exchange by various mesons (realistic potentials [18, 19]) or presented as model functions whose parameters are found from the description of observables in the elastic neutron-proton (np) scattering (separable [20]-[26], phenomenological [27] models etc). There are also alternative approaches [7, 15, 16], relativistic quantum mechanics, which are based on the Hamiltonian approach.

From the viewpoint of simplicity of performing calculations presentation of interaction in a separable form is the most convenient instrument [17]. That is why there are separable approximations intended only to reproduce the behavior of the corresponding realistic potentials and used in calculations instead of more complicated originals (see, for example, [18] and [25]). However, the construction of presentations of this type is a complicated problem. The first elaborated models [20, 21] were nonrelativistic and, therefore, they were of little use for the description of reactions with high-energy particles. In addition, there were problems with their off-shell behavior, see, for example [22, 23]. This behavior was adjusted in subsequent models [24]-[26] by fitting to the corresponding realistic potentials using the Ernst-Shakin-Thaler method [28]. However, all these models do not contain the zero component of the momentum of considered particles which is necessary to construct a covariant model. One of the attempts of this kind is [29] where the relativistically generalized version of Graz II potential [24] was proposed. It describes the experimental data for the laboratory energies of the colliding neutron and proton T_{Lab} up to 0.5 GeV. However, its application is limited in principle because of nonintegrability of expressions containing the constructed form factors [17] at higher T_{Lab} . The problem can be solved by using the modified form factors [30]. This idea was developed in [31]-[34] for the description of uncoupled partial-wave states in the elastic np scattering for T_{Lab} up to 3 GeV.

In the present paper the separable interaction kernel for the triplet partial-wave state 3S_1 - 3D_1 is proposed. The work is a continuation of the previous

one [34] where the uncoupled partial-wave states with the total angular momenta $J = 0, 1$ were considered. Investigations of various deuteron characteristics are performed using the elaborated kernel. Parameters of the model are defined from the calculations of experimental data for phase shifts taken from the SAID program (<http://gwdac.phys.gwu.edu>) and low-energy characteristics. The off-shell behavior of the kernel is compared with the deuteron wave function and the Noyes-Kowalski function [35, 36] obtained for some realistic potentials (here Paris, CD-Bonn) which are very good at low energies.

The paper is organized as follows. In Sec. 2, the general Bethe-Salpeter formalism used for the description of the np system is considered. In Sec. 3, the solution of the BS equation using the separable presentation of its kernel is discussed. The proposed model is expounded in Sec. 4. The calculations of introduced parameters and obtained low-energy deuteron characteristics are presented in Sec. 5. The review of the results for phase shifts of the elastic np scattering, components of the Noyes-Kowalski function, deuteron wave function and the conclusions are given in Sec. 6.

2. Bethe-Salpeter formalism

In the relativistic field theory, elastic nucleon-nucleon (NN) scattering can be described by the scattering matrix T which satisfies the inhomogeneous Bethe-Salpeter equation [37]. In momentum space, the BS equation for the T matrix can be (in terms of the relative four-momenta p' and p and the total four-momentum P) represented as:

$$T(p', p; P) = V(p', p; P) + \frac{i}{4\pi^3} \int d^4k V(p', k; P) S_2(k; P) T(k, p; P), \quad (1)$$

where $V(p', p; P)$ is the interaction kernel and $S_2(k; P)$ is the free two-particle Green function

$$S_2^{-1}(k; P) = \left(\frac{1}{2} P \cdot \gamma + k \cdot \gamma - m\right)^{(1)} \left(\frac{1}{2} P \cdot \gamma - k \cdot \gamma - m\right)^{(2)},$$

γ are the Dirac gamma-matrices. The square of the total momentum $s = (p_1 + p_2)^2$ and the relative momentum $p = (p_1 - p_2)/2$ [$p' = (p'_1 - p'_2)/2$] are defined via the nucleon momenta p_1, p_2 [p'_1, p'_2] of initial [final] nucleons.

Performing the partial-wave decomposition (see details in [17, 34]) of the T matrix and interaction kernel V we can rewrite the BS equation for the

off-shell partial-wave amplitudes:

$$\begin{aligned}
T_{ab}(p'_0, |\mathbf{p}'|; p_0, |\mathbf{p}|; s) &= V_{ab}(p'_0, |\mathbf{p}'|; p_0, |\mathbf{p}|; s) \\
&+ \frac{i}{4\pi^3} \sum_{cd} \int_{-\infty}^{+\infty} dk_0 \int_0^{\infty} \mathbf{k}^2 d|\mathbf{k}| V_{ac}(p'_0, |\mathbf{p}'|; k_0, |\mathbf{k}|; s) \\
&\times S_{cd}(k_0, |\mathbf{k}|; s) T_{db}(k_0, |\mathbf{k}|; p_0, |\mathbf{p}|; s).
\end{aligned} \tag{2}$$

Here indices a, b etc denote the corresponding partial-wave state quantum numbers $|aM\rangle \equiv |\pi, {}^{2S+1}L_J^\rho M\rangle$ [38], where S is the total spin, L is the orbital angular momentum, and J is the total angular momentum with the projection M ; relativistic quantum numbers ρ and π refer to the relative-energy and spatial parity with respect to the change of sign of the relative energy and spatial vector, respectively. The two-spinor propagator S_{ab} depends only on ρ -spin indices. The quantum number ρ defines the positive- ($\rho = +$) or negative-energy ($\rho = -$) partial-wave states. In nonrelativistic models of nuclear-nuclear interactions only positive-energy states are considered; therefore, ρ is superfluous to be shown as a quantum number. In the relativistic model the $\rho = -$ states should be described in the general case. However, since only positive-energy partial states are considered in the paper below ρ is omitted.

Calculating the T matrix we can connect the parameters of the BS kernel V with observables. For the description of the T matrix we use the following normalization condition in the on-mass-shell form for the triplet state:

$$T_{ll}(s) = \frac{i8\pi}{\sqrt{s}\sqrt{s-4m^2}} \begin{pmatrix} \cos 2\varepsilon_1 e^{2i\delta_<} - 1 & i \sin 2\varepsilon_1 e^{i(\delta_<+\delta_>)} \\ i \sin 2\varepsilon_1 e^{i(\delta_<+\delta_>)} & \cos 2\varepsilon_1 e^{2i\delta_>} - 1 \end{pmatrix}, \tag{3}$$

where m is a nucleon mass and ε_1 is a mixing parameter. In Eq.(3) $\delta_< = \delta_{L=J-1}$, $\delta_> = \delta_{L=J+1}$ and l denotes ${}^{2S+1}L_J$ states for simplicity. Expanding the T matrix into a series of \bar{p} -terms, according to [39],

$$\bar{p} \cot \delta_l(s) = -\frac{1}{a_0^l} + \frac{r_0^l}{2} \bar{p}^2 + \mathcal{O}(\bar{p}^3), \tag{4}$$

where

$$\bar{p} \equiv |\bar{\mathbf{p}}| = \sqrt{s/4 - m^2} = \sqrt{mT_{\text{Lab}}/2} \tag{5}$$

is the on-mass-shell momentum, one can derive low-energy parameters, the scattering length a_0 and the effective range r_0 .

The bound state of the two-particle system appears as a simple pole in the T matrix at $s = M_d^2$, with M_d being a mass of a bound state, in our case it is a deuteron. Thus, the Bethe-Salpeter equation for the BS amplitude Φ of the two-nucleon system with the total momentum J and its projection M has the following form:

$$\Phi^{JM}(p; P) = \frac{i}{(2\pi)^4} S_2(p; P) \int d^4k V(p, k; P) \Phi^{JM}(k; P), \quad (6)$$

The partial-wave decomposed amplitude Φ can be written in the rest frame of the particles through the generalized spherical harmonic \mathcal{Y} and the radial ϕ part as:

$$\Phi_{\alpha\beta}^{JM}(p; P_{(0)}) = \sum_a (\mathcal{Y}_{aM}(\mathbf{p}) U_C)_{\alpha\beta} \phi_a(p_0, |\mathbf{p}|; s), \quad (7)$$

where $P_{(0)} = (M_d, \mathbf{0})$ is the total momentum of the NN system in its rest frame. Here U_C is the charge conjugation matrix. In the numerical calculations instead of the amplitude it is more convenient to use the vertex function Γ which is connected with the BS amplitude:

$$\Phi_{JM}(p; P) = S_2(p; P) \Gamma_{JM}(p; P), \quad (8)$$

so the radial parts of the BS amplitude ϕ and the vertex function g are connected by the relation:

$$\phi_a(p_0, |\mathbf{p}|) = \sum_b S_{ab}(p_0, |\mathbf{p}|; s) g_b(p_0, |\mathbf{p}|). \quad (9)$$

To solve the equations for the T matrix and BS amplitude, one should use some assumption for the kernel V . In our case it is a separable ansatz.

3. Separable model

We assume that the interaction conserves parity, total angular momentum J and its projection, and isotopic spin. Due to the NN tensor force, the orbital angular momentum L is not conserved. Moreover, the negative-energy two-nucleon states are omitted, which leads to the total spin S conservation. The partial-wave-decomposed BS equation is therefore reduced to the

following form:

$$T_{\nu l}(p'_0, |\mathbf{p}'|; p_0, |\mathbf{p}|; s) = V_{\nu l}(p'_0, |\mathbf{p}'|; p_0, |\mathbf{p}|; s) \quad (10)$$

$$+ \frac{i}{4\pi^3} \sum_{\nu''} \int_{-\infty}^{+\infty} dk_0 \int_0^{\infty} \mathbf{k}^2 d|\mathbf{k}| \frac{V_{\nu \nu''}(p'_0, |\mathbf{p}'|; k_0, |\mathbf{k}|; s) T_{\nu'' l}(k_0, |\mathbf{k}|; p_0, |\mathbf{p}|; s)}{(\sqrt{s}/2 - E_{\mathbf{k}} + i\epsilon)^2 - k_0^2}.$$

Supposing the separable (rank- N) ansatz for V :

$$V_{\nu l}(p'_0, |\mathbf{p}'|; p_0, |\mathbf{p}|; s) = \sum_{i,j=1}^N \lambda_{ij}(s) g_i^{[\nu]}(p'_0, |\mathbf{p}'|) g_j^{[l]}(p_0, |\mathbf{p}|), \quad (11)$$

where the form factors $g_j^{[l]}$ represent the model functions, we can obtain the solution of Eq.(10) in a similar separable form for the T matrix:

$$T_{\nu l}(p'_0, |\mathbf{p}'|; p_0, |\mathbf{p}|; s) = \sum_{i,j=1}^N \tau_{ij}(s) g_i^{[\nu]}(p'_0, |\mathbf{p}'|) g_j^{[l]}(p_0, |\mathbf{p}|), \quad (12)$$

where

$$\tau_{ij}(s) = 1/(\lambda_{ij}^{-1}(s) + h_{ij}(s)), \quad (13)$$

$$h_{ij}(s) = -\frac{i}{4\pi^3} \sum_l \int dk_0 \int \mathbf{k}^2 d|\mathbf{k}| \frac{g_i^{[l]}(k_0, |\mathbf{k}|) g_j^{[l]}(k_0, |\mathbf{k}|)}{(\sqrt{s}/2 - E_{\mathbf{k}} + i\epsilon)^2 - k_0^2}, \quad (14)$$

$\lambda_{ij}(s)$ is a matrix of model parameters with the symmetry property:

$$\lambda_{ij}(s) = \lambda_{ji}(s). \quad (15)$$

Using the separable ansatz (11) and performing the partial-wave decomposition for the interaction kernel and vertex function we can represent the radial part of the latter as follows:

$$g_l(p_0, |\mathbf{p}|) = \sum_{i,j=1}^N \lambda_{ij}(s) g_i^{[l]}(p_0, |\mathbf{p}|) c_j(s), \quad (16)$$

where $l = S(D)$ corresponds to the ${}^3S_1({}^3D_1)$ wave in the deuteron, and the integral equation (6) is reduced to a system of linear homogeneous equations for the coefficients $c_i(s)$:

$$c_i(s) - \sum_{k,j=1}^N h_{ik}(s)\lambda_{kj}(s)c_j(s) = 0. \quad (17)$$

The radial part of the BS amplitude has the form (see Eq.(9)):

$$\phi_l(p_0, |\mathbf{p}|) = \frac{g_l(p_0, |\mathbf{p}|)}{(M_d/2 - E_{\mathbf{p}} + i\epsilon)^2 - p_0^2}. \quad (18)$$

The form factors $g_i^{[l]}$ used in the separable representation (11) are obtained by a relativistic generalization of the initially nonrelativistic Yamaguchi-type functions depending on the three-dimensional squared momentum $|\mathbf{p}|$. Methods of covariant relativistic generalizations and the constructed form factors are discussed in the next section.

4. Construction of the covariant separable kernel

We consider two types of a relativistic generalization of nonrelativistic Yamaguchi-type form factors [40] performing the following changes:

$$\mathbf{p}^2 \rightarrow -p^2 = -p_0^2 + \mathbf{p}^2 \quad (19)$$

$$\text{or} \quad \mathbf{p}^2 \rightarrow Q^2 : Q = p - \frac{P \cdot p}{s} P \quad (20)$$

and denote the resulting modified form factors of the constructed rank-six interaction kernels by MY6 (19), MYQ6 (20). So high rank is necessary to describe simultaneously phase shifts for two waves and bound state characteristics in addition to usual low-energy parameters. The form factors have the following form:

$$\begin{aligned} g_1^{[S]}(p) &= \frac{(p_{c1} - p_0^2 + \mathbf{p}^2)}{(p_0^2 - \mathbf{p}^2 - \beta_1^2)^2 + \alpha_1^4}, \\ g_2^{[S]}(p) &= \frac{(p_0^2 - \mathbf{p}^2)(p_{c2} - p_0^2 + \mathbf{p}^2)^2}{((p_0^2 - \mathbf{p}^2 - \beta_2^2)^2 + \alpha_2^4)^2}, \\ g_3^{[S]}(p) &= \frac{(p_0^2 - \mathbf{p}^2)^3(p_{c3} - p_0^2 + \mathbf{p}^2)^2}{((p_0^2 - \mathbf{p}^2 - \beta_3^2)^2 + \alpha_3^4)^3}, \end{aligned} \quad (21)$$

$$g_4^{[S]} = g_5^{[S]} = g_6^{[S]} = g_1^{[D]} = g_2^{[D]} = g_3^{[D]} = 0, \quad (22)$$

$$g_4^{[D]}(p) = \frac{-(p_0^2 - \mathbf{p}^2)(p_{c4} - p_0^2 + \mathbf{p}^2)^2}{((p_0^2 - \mathbf{p}^2 - \beta_{41}^2)^2 + \alpha_{41}^4)((p_0^2 - \mathbf{p}^2 - \beta_{42}^2)^2 + \alpha_{42}^4)}, \quad (23)$$

$$g_5^{[D]}(p) = \frac{-(p_0^2 - \mathbf{p}^2)}{(p_0^2 - \mathbf{p}^2 - \beta_5^2)^2 + \alpha_5^4},$$

$$g_6^{[D]}(p) = \frac{(p_0^2 - \mathbf{p}^2)^4(p_{c6} - p_0^2 + \mathbf{p}^2)}{((p_0^2 - \mathbf{p}^2 - \beta_{61}^2)^2 + \alpha_{61}^4)((p_0^2 - \mathbf{p}^2 - \beta_{62}^2)^2 + \alpha_{62}^4)}.$$

The functions for the model approximation MYQ6 can be obtained from (21)-(23) by the change $p^2 \rightarrow Q^2$. The detailed discussion of properties of the presented form factors can be found in [32]-[34].

Due to the structure of the separable presentation, Eqs.(21)-(23), the matrix $H = \{h_{ij}\}$ (14) can be written as

$$H(s) = \begin{pmatrix} h_{11}(s) & h_{12}(s) & h_{13}(s) & 0 & 0 & 0 \\ h_{12}(s) & h_{22}(s) & h_{23}(s) & 0 & 0 & 0 \\ h_{13}(s) & h_{23}(s) & h_{33}(s) & 0 & 0 & 0 \\ 0 & 0 & 0 & h_{44}(s) & h_{45}(s) & h_{46}(s) \\ 0 & 0 & 0 & h_{45}(s) & h_{55}(s) & h_{56}(s) \\ 0 & 0 & 0 & h_{46}(s) & h_{56}(s) & h_{66}(s) \end{pmatrix}. \quad (24)$$

The solution of the BS equation for the radial parts of the vertex function can be expressed through the introduced form factors with the help of Eqs.(9), (16), (17). To fix the coefficients c_i which are solutions of a system of linear homogeneous equations, we use the normalization condition for the 3S_1 and 3D_1 states:

$$p_S + p_D = 1, \quad (25)$$

where the pseudoprobabilities of these waves are introduced:

$$p_l = \frac{i}{2M_d(2\pi)^4} \int dp_0 \int \mathbf{p}^2 d|\mathbf{p}| \frac{(E_{\mathbf{p}} - M_d/2)[g_l(p_0, |\mathbf{p}|)]^2}{((M_d/2 - E_{\mathbf{p}} + i\epsilon)^2 - p_0^2)^2}, \quad (26)$$

The resulting coefficients c_i are presented in Table 1.

The half-off-shell behavior of the interaction is controlled by the Noyes-Kowalski function [35, 36] in the pair rest frame (c.m.) where the corresponding partial-wave decomposition of the T matrix [17] is performed:

$$f_{\nu l}(p; \bar{p}) = \frac{T_{\nu l}(0, |\mathbf{p}|; 0, |\bar{\mathbf{p}}|; s)}{T_{\nu l}(0, |\bar{\mathbf{p}}|; 0, |\bar{\mathbf{p}}|; s)} \quad (27)$$

and compared with the Paris [18] potential and relativistic Graz II model [29]. Here $\bar{\mathbf{p}}$ (5) is the on-shell and \mathbf{p} is the off-shell momenta, respectively. It should be noted that there are three different variants of the Graz II separable presentation of the BS kernel differing by the D wave probability. We choose the variant with $p_D = 5\%$.

We also constrain the parameters of the separable interaction so that our model reproduces the deuteron asymptotic D/S ratio

$$\rho_{D/S} = \frac{g_D(0, p^*)}{g_S(0, p^*)}, \quad (28)$$

where $p^{*2} = -mE_d$. Finally, the deuteron magnetic moment μ_d is not included in the fit and is calculated as it is.

Table 1: Coefficients c_i .

	MY6	MYQ6
c_1	0.0486061704	0.0704040072
c_2	0.00225058402	0.00453017913
c_3	-0.00671506834	-0.171434026
c_4	-0.019764894	0.0080399654
c_5	0.00277839389	0.00618413506
c_6	-0.304144129	0.0682392337

5. Calculations and results

Using the np scattering data we analyze the parameters of the constructed separable models. A pole in the T matrix at the mass of the bound state M_d :

$$\det |\tau_{ij}^{-1}(s = M_d^2)| = 0 \quad (29)$$

is taken into account by introducing the additional parameter m_0 :

$$\lambda_{ij}(s) = \frac{\bar{\lambda}_{ij}}{s - m_0^2}. \quad (30)$$

The parameter m_0 is chosen to satisfy the following condition:

$$\bar{\lambda}_{ij}^{-1}(s - m_0^2) + h_{ij}(M_d^2) = 0, \quad (31)$$

where $M_d = (2m - E_d)$ and E_d is the energy of the deuteron.

The calculation of the parameters is performed by using Eqs.(3),(4) and expressions given to reproduce experimental values for all available data from the SAID program (<http://gwdac.phys.gwu.edu>) for phase shifts. The low-energy scattering parameters are taken from [41].

The calculations are performed using the Wick rotation [42]. All integrals are calculated numerically with the technique elaborated in [45].

The introduced free parameters are found from the minimization of the χ^2 function. The asymptotic ratio $\rho_{D/S}$ is also taken into account in the minimization procedure. The phase shifts for S and D waves are both included in one minimization function:

$$\begin{aligned} \chi^2 = & \\ & \sum_{i=1}^n (\delta_{<}^{\text{exp}}(s_i) - \delta_{<}(s_i))^2 / (\Delta\delta_{<}^{\text{exp}}(s_i))^2 + (\delta_{>}^{\text{exp}}(s_i) - \delta_{>}(s_i))^2 / (\Delta\delta_{>}^{\text{exp}}(s_i))^2 \\ & + (a^{\text{exp}} - a)^2 / (\Delta a^{\text{exp}})^2 + (\rho_{D/S}^{\text{exp}} - \rho_{D/S})^2 / (\Delta\rho_{D/S}^{\text{exp}})^2. \end{aligned} \quad (32)$$

Here n is a number of experimental points.

The effective range r_0 is calculated via the obtained parameters and compared with the experimental value r_0^{exp} .

The calculated parameters of the separable presentations MY6 and MYQ6 are listed in Tables 2 and 3, respectively. In Table 4, the calculated low-energy scattering parameters and deuteron characteristics are compared with the corresponding experimental values and other models (Graz II [29], Paris [18], CD-Bonn [46]).

In Figs.1 and 2, the results of the phase shift calculations are compared with experimental data and, in addition to the afore-said theoretical models, with the empirical SP07 SAID solution [47]. The mixing parameter is pictured in Fig.3. As an example of comparison with a separable model we take here the nonrelativistic Graz II [24] potential model (denoted by Graz II (NR)). The comparison with the relativistic interaction kernel Graz II [29] is not presented because using it the phase shifts and the mixing parameter cannot be calculated in the whole energy range where these observables are known. As it was discussed in [17, 34], in this case when T_{Lab} exceeds some

limit value depending on the parameters in separable form factors it is impossible to perform numerical calculations in principle, whereas our aim is to compare our MY6 and MYQ6 with results of other models in a wide energy range. Wherever it is possible to use the relativistic Graz II at high energies we make a comparison with it.

The obtained components of the Noyes-Kowalski function (27) are presented in Figs.4-7. The S - and D -state wave functions $\phi(\bar{p}_0, \mathbf{p})$ (18), where $\bar{p}_0 = M_d/2 - E_{\mathbf{p}}$ [48], are given in Figs.8 and 9, respectively, and compared with the corresponding relativistic and nonrelativistic Graz II models and the Paris potential [18].

As an illustration of the behavior of the elaborated separable models when reactions with the deuteron are considered, in Figs.10-12, the results of calculations of cross sections for the deuteron electrodisintegration within the relativistic plane-wave impulse approximation are presented. We compare the obtained results for the differential cross section with those obtained earlier [49] using the relativistic Graz II model [29] for three different kinematic cases [50, 51].

Table 2: Parameters of the rank-six separable model with modified (19) Yamaguchi functions MY6.

MY6			
$\bar{\lambda}_{11}$ (GeV ²)	-126.823	β_1 (GeV)	0.1000189
$\bar{\lambda}_{12}$ (GeV ²)	-1627.106	β_2 (GeV)	1.2089089
$\bar{\lambda}_{13}$ (GeV ²)	-78.78723	β_3 (GeV)	0.3884728
$\bar{\lambda}_{14}$ (GeV ²)	1255.789	β_{41} (GeV)	0.1617235
$\bar{\lambda}_{15}$ (GeV ²)	1920.741	β_{42} (GeV)	1.0569099
$\bar{\lambda}_{16}$ (GeV ²)	23.25852	β_5 (GeV)	0.5975024
$\bar{\lambda}_{22}$ (GeV ²)	-1507.037	β_{61} (GeV)	0.1000189
$\bar{\lambda}_{23}$ (GeV ²)	-202.4665	β_{62} (GeV)	0.2562457
$\bar{\lambda}_{24}$ (GeV ²)	-1211.809	α_1 (GeV)	1.7190386
$\bar{\lambda}_{25}$ (GeV ²)	19296.73	α_2 (GeV)	1.1342682
$\bar{\lambda}_{26}$ (GeV ²)	-19.71478	α_3 (GeV)	0.7779747
$\bar{\lambda}_{33}$ (GeV ²)	-4.911057	α_{41} (GeV)	0.1143112
$\bar{\lambda}_{34}$ (GeV ²)	52.90785	α_{42} (GeV)	1.9584773
$\bar{\lambda}_{35}$ (GeV ²)	-557.975	α_5 (GeV)	10.71719
$\bar{\lambda}_{36}$ (GeV ²)	-5.781583	α_{61} (GeV)	0.1743705
$\bar{\lambda}_{44}$ (GeV ²)	2388.451	α_{62} (GeV)	0.3825411
$\bar{\lambda}_{45}$ (GeV ²)	1481.914	p_{c1} (GeV ²)	-3.947706
$\bar{\lambda}_{46}$ (GeV ²)	23.63605	p_{c2} (GeV ²)	-29.997902
$\bar{\lambda}_{55}$ (GeV ²)	-47615.28	p_{c3} (GeV ²)	3.9076391
$\bar{\lambda}_{56}$ (GeV ²)	314.5085	p_{c4} (GeV ²)	0.5632583
$\bar{\lambda}_{66}$ (GeV ²)	1.135512	p_{c6} (GeV ²)	0.278038
m_0 (GeV)	1.350753		

Table 3: Parameters of the rank-six separable model with modified (20) Yamaguchi functions MYQ6.

MYQ6			
$\bar{\lambda}_{11}$ (GeV ²)	-10.574	β_1 (GeV)	0.100019
$\bar{\lambda}_{12}$ (GeV ²)	-3498.482	β_2 (GeV)	0.5978559
$\bar{\lambda}_{13}$ (GeV ²)	2.031008	β_3 (GeV)	0.431291
$\bar{\lambda}_{14}$ (GeV ²)	98.12	β_{41} (GeV)	0.210503
$\bar{\lambda}_{15}$ (GeV ²)	31.318	β_{42} (GeV)	0.1001783
$\bar{\lambda}_{16}$ (GeV ²)	-30.813	β_5 (GeV)	5.5725
$\bar{\lambda}_{22}$ (GeV ²)	10548.08	β_{61} (GeV)	0.1120488
$\bar{\lambda}_{23}$ (GeV ²)	-76.928	β_{62} (GeV)	0.4489458
$\bar{\lambda}_{24}$ (GeV ²)	-3720.413	α_1 (GeV)	1.468872
$\bar{\lambda}_{25}$ (GeV ²)	37427.57	α_2 (GeV)	1.09121
$\bar{\lambda}_{26}$ (GeV ²)	-208.697	α_3 (GeV)	0.7449097
$\bar{\lambda}_{33}$ (GeV ²)	0.77	α_{41} (GeV)	0.1
$\bar{\lambda}_{34}$ (GeV ²)	-22.51814	α_{42} (GeV)	1.945662
$\bar{\lambda}_{35}$ (GeV ²)	-84.478	α_5 (GeV)	4.08
$\bar{\lambda}_{36}$ (GeV ²)	2.1435	α_{61} (GeV)	0.2058123
$\bar{\lambda}_{44}$ (GeV ²)	895.2475	α_{62} (GeV)	0.7052189
$\bar{\lambda}_{45}$ (GeV ²)	286.5565	p_{c1} (GeV ²)	-4.2035
$\bar{\lambda}_{46}$ (GeV ²)	19.419	p_{c2} (GeV ²)	-13.82
$\bar{\lambda}_{55}$ (GeV ²)	-32435.14	p_{c3} (GeV ²)	9.574
$\bar{\lambda}_{56}$ (GeV ²)	-705.156	p_{c4} (GeV ²)	1.152
$\bar{\lambda}_{66}$ (GeV ²)	-21.792	p_{c6} (GeV ²)	-0.4527
m_0 (GeV)	1.351914		

Table 4: The low-energy scattering parameters for the triplet 3S_1 - 3D_1 state and the deuteron characteristics.

	a_{0t} (fm)	r_{0t} (fm)	p_D (%)	E_d (MeV)	$\rho_{D/S}$	μ_d ($e/2m$)
MY6	5.42	1.800	4.92	2.2246	0.0255	0.8500 ^a
MYQ6	5.42	1.768	4.65	2.2246	0.0259	0.8535 ^a
Graz II	5.42	1.779	5	2.2254	0.0269	0.8512
Paris	5.43	1.770	5.77	2.2249	0.0261	0.8469
CD-Bonn	5.4196	1.751	4.85	2.2246	0.0256	0.8522
Exp.	5.424(4)	1.759(5)	4-7	2.224644(46)	0.0256(4) ^b	0.8574 ^c

^a Calculated within the relativistic impulse approximation with the positive-energy partial-wave states only.

^b Ref. [43].

^c Ref. [44].

6. Discussion and conclusions

The first step in construction of the interaction kernel in a separable form is the description of on-mass-shell characteristics, like phase shifts, low-energy characteristics, and the mixing parameter. In Figs.1 and 2, the results of our calculations of phase shifts for the 3S_1 and 3D_1 waves are presented. Figure 1 demonstrates that the 3S_1 partial-wave state is well described by both MY6 and MYQ6 parametrizations for all experimental data. The Graz II (NR) works for $T_{\text{Lab}} \leq 0.4$ GeV. For the 3D_1 state MY6 and MYQ6 provide a good description of existing data. Graz II (NR) shows only some correspondence with the data for $T_{\text{Lab}} \leq 0.4$ GeV. SP07 is good for all experimental data. CD-Bonn was constructed for $T_{\text{Lab}} \leq 350$ MeV and is perfect in this region. Its behavior means that other models should be used for higher energies, whereas the interaction kernels MY6 and MYQ6 allow to perform calculations in this case.

The problem of simultaneous description of phase shifts for the coupled partial-wave states, the mixing parameter and the low-energy and deuteron characteristics is worthy of a special discussion. This subject was considered in detail in [24]. The authors found out that an attempt to describe well the mixing parameter together with other observables leads to very bad results for the low-energy and deuteron parameters. They become too small in comparison with permissible values, in particular $p_D \lesssim 1\%$. It should be noted

that our investigation of interaction kernels of a rank ≤ 6 demonstrated that increasing in a rank does not result in a better description of ε_1 . Performing numerical investigations we discovered the same properties. In most cases there is no possibility to reproduce phase shifts, low-energy parameters, and mixing parameter simultaneously. A certain advance was achieved in the CD-Bonn potential model where the mixing parameter behavior looks very good for kinetic energies till about 350 MeV for Nijmegen group analysis [52]. Although there are SAID group data [47] which differ from Nijmegen group ones this is the best result for the moment. However, taking into account this discrepancy in the analysis of the experimental data for the mixing parameter we restrict ourselves to the description of all observables but ε_1 . At the same time, for completeness we present the obtained results for ε_1 along with the results of all other discussed models (Fig.3). It can be seen that both elaborated models do not work at all like Graz II (NR) potential which also does not give any agreement with the data. SP07 agrees with the experiment in the whole energy range.

The half-off-shell behavior characterized by the Noyes-Kowalski function (27) was not fitted in any special way, it was simply calculated as it is. In Figs.4-7, all components of this function are presented. The obtained MY6 and MYQ6 functions are similar but not identical to the Graz II potential functions. The same can be said about diagonal components of the function for the realistic Paris potential, whereas the difference for non-diagonal components is significant. In addition, MY6 modification is not identical to MYQ6 one. This difference should affect observables defined by the half-off-shell behavior of the described interaction, especially various polarizations [53].

As any other phenomenological model ours can describe on-shell characteristics quite easily. However, the description of the coupled 3S_1 - 3D_1 channel is not limited only by phase shifts and low-energy observables. It is also important to look at properties of the deuteron BS amplitude (wave function). Therefore, in calculations we take into account features of the wave functions corresponding to 3S_1 and 3D_1 parts. In Figs.8 and 9, it is shown that the obtained functions are similar to other discussed models in the energy region where their properties play a key role.

As an example of using the interaction kernels constructed in this paper we calculate the differential cross sections [49] within the simplest relativistic plane-wave impulse approximation for various kinematic conditions [50, 51] and compare them with the corresponding relativistic Graz II model [29] cal-

culations. From Figs.10-12, it can be seen that the presented results begin to differ only when the influence of the D wave increases. However, to make a conclusion it is necessary to take into account other effects, like the final state interaction (FSI) and two-body currents. This was impossible before because of problems with calculations, as it was discussed in [34]. Now these difficulties are obviated and it is planned to perform calculations of observables with FSI using the elaborated model and the results of our previous work [34] in near future.

In conclusion, it can be said that the constructed rank-six interaction kernels were successfully used for the description of the on-shell and off-shell characteristics of the triplet 3S_1 - 3D_1 partial-wave state of the np system and the deuteron. Good agreement with results of other models which work at low energies for phase shifts, low-energy parameters, deuteron wave function was achieved. The demonstrated half-off-shell behavior is similar to the corresponding Graz II model. The constructed separable model of NN interaction can be used in calculations of various reactions with the deuteron, e.g., the deuteron photo- and electrodisintegration etc. It is also interesting to investigate the elastic electron-deuteron scattering process using this new model. However, it is a subject of a separate work.

Additional parameters α provide integrands containing form factors of the separable presentation to have no poles for \mathbf{p} component. Therefore, in particular, using this type of functions for form factors will make numerical calculations of the electrodisintegration far from the threshold possible without resorting quasipotential or nonrelativistic approximations. A comparison with other separable and realistic potential models allows us to demonstrate merits of separable kernels with α -modified form factors. For example, the CD-Bonn potential, which was constructed for $T_{\text{Lab}} \leq 350$ MeV and works in this energy interval very well, cannot just be simply extrapolated at higher energies. As for the Graz II interaction kernel, the increase in energies of the considered particles is impossible in principle. On the contrary, our model has no these limitations. We do not describe the mixing parameter; nevertheless, all low-energy and deuteron characteristics are reproduced well and the results for phase shifts cover the whole energy region and are of high quality. Finally, we have no insuperable obstacles in calculations and there is an opportunity to improve the model in future.

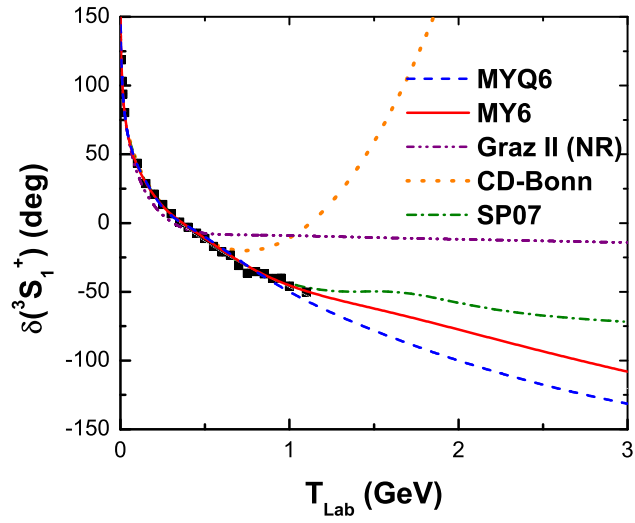


Figure 1: The model phase shifts for the 3S_1 and for two relativistic separable kernel cases MY6 and MYQ6 are compared to those of Graz II (NR) [24], CD-Bonn [46] and of the empirical SP07 SAID solution [47].

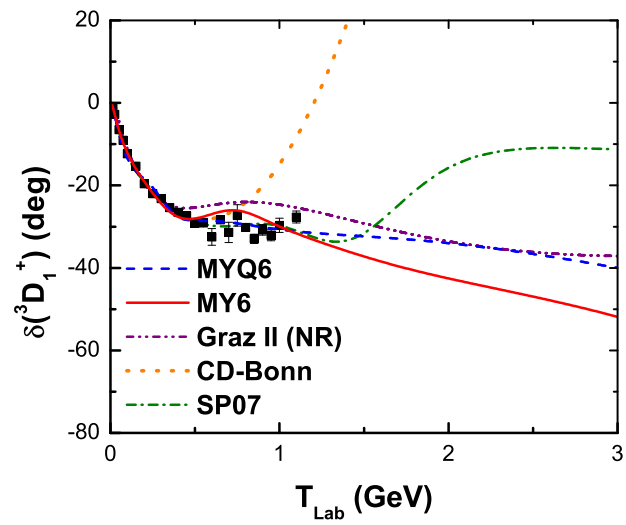


Figure 2: As in Fig.1, but for the 3D_1 wave.

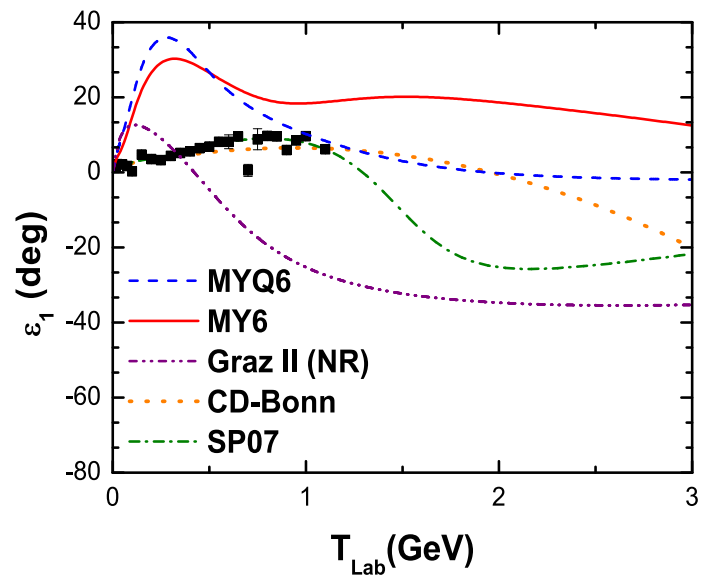


Figure 3: As in Fig.1, but for the mixing parameter.

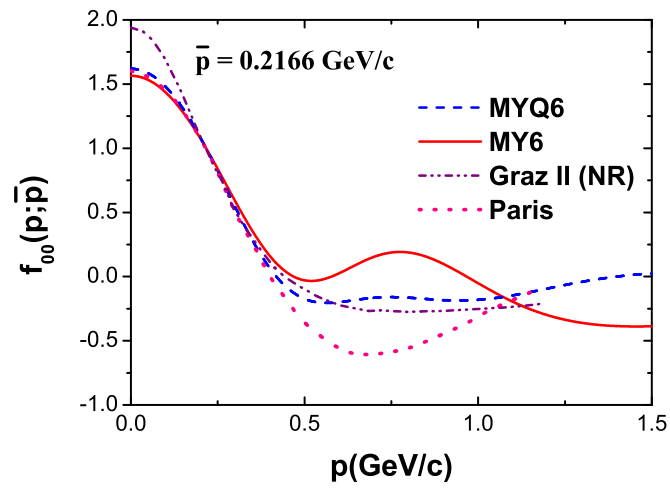


Figure 4: The Noyes-Kowalski function f_{00} in c.m. for two relativistic separable kernel cases MY6 and MYQ6 is compared to those of the separable Graz II (NR) [24] and realistic Paris [18] potentials.

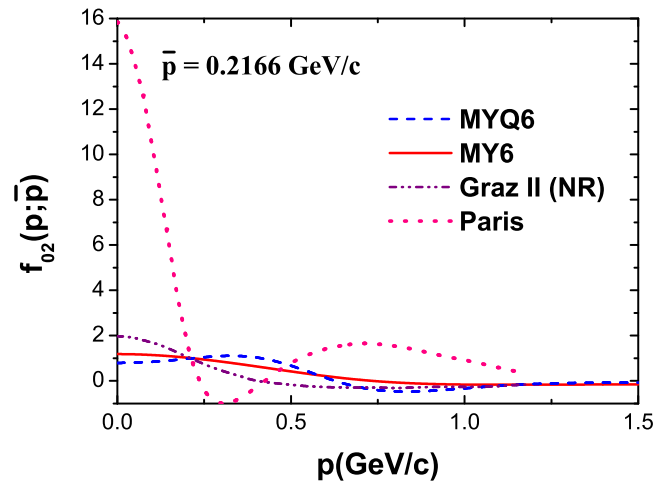


Figure 5: As in Fig.4, but for the component f_{02} of the Noyes-Kowalski function.

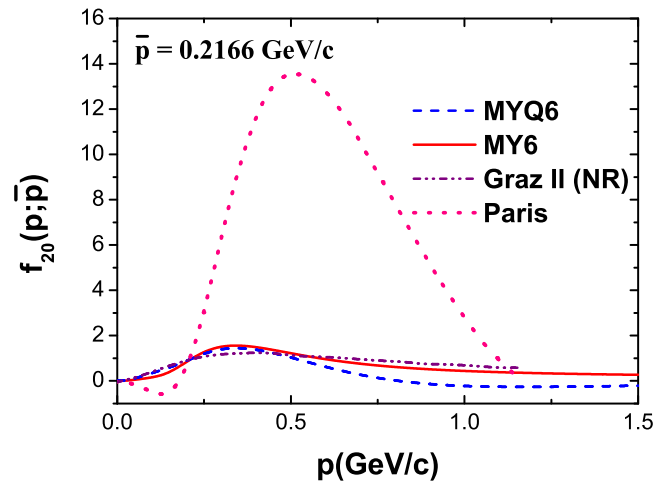


Figure 6: As in Fig.4, but for the component f_{20} of the Noyes-Kowalski function.

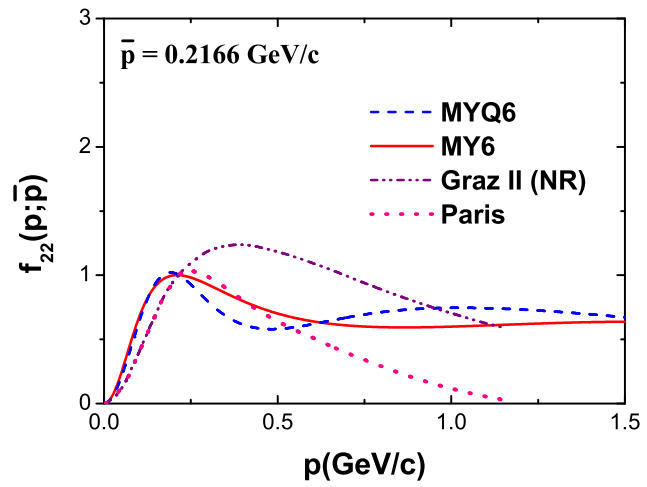


Figure 7: As in Fig.4, but for the component f_{22} of the Noyes-Kowalski function.

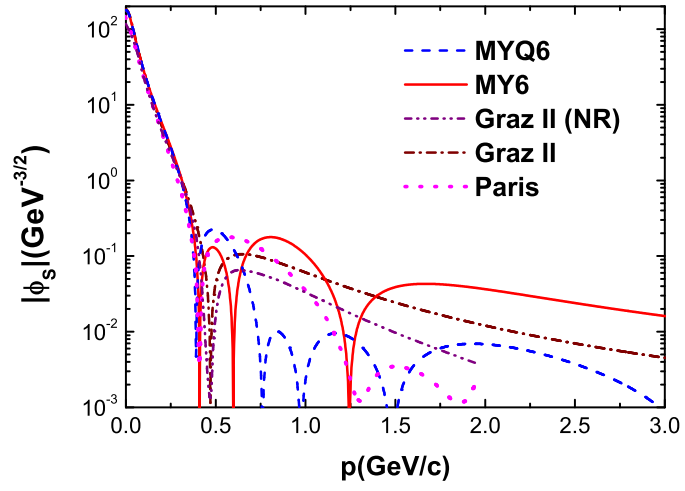


Figure 8: The wave function for the 3S_1 partial-wave state in the deuteron rest frame for the MY6 and MYQ6 models in comparison with those of Graz II (NR) [24], Graz II [29] and Paris [18].

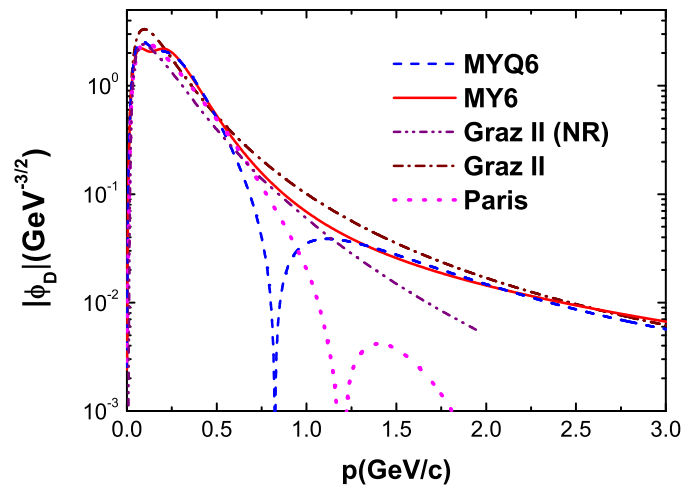


Figure 9: As in Fig.8, but for the 3D_1 partial-wave state.

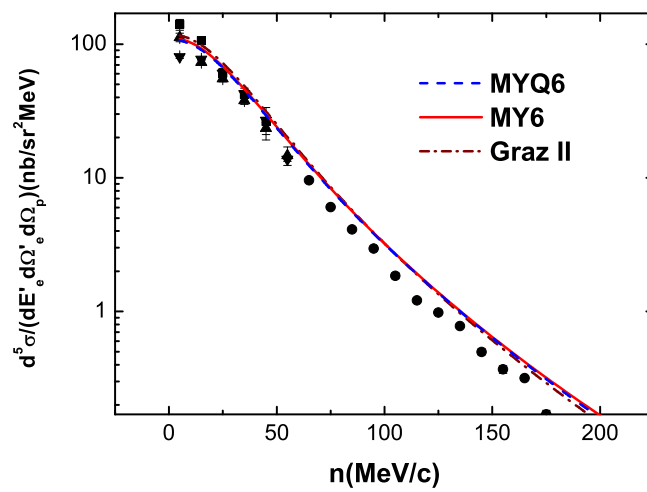


Figure 10: Cross section for the $d(e,e'p)n$ reaction, kinematical conditions set I [50]. n is the recoil momentum of the final neutron. The detailed discussion of the considered observable can be found in [49].

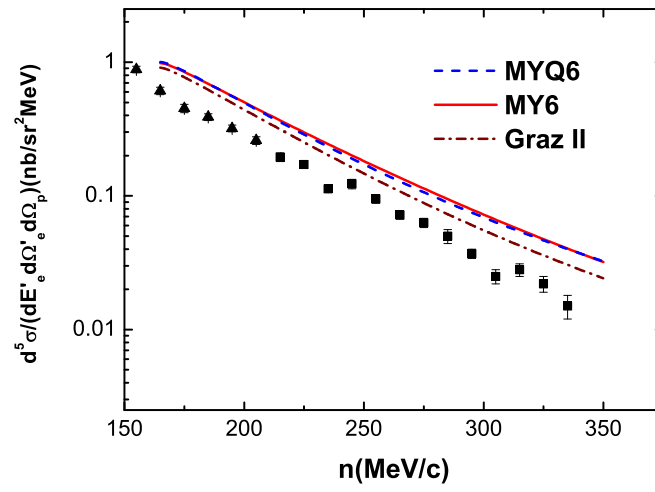


Figure 11: Cross section for the kinematical conditions set II [50]. See also the caption of Fig.10.

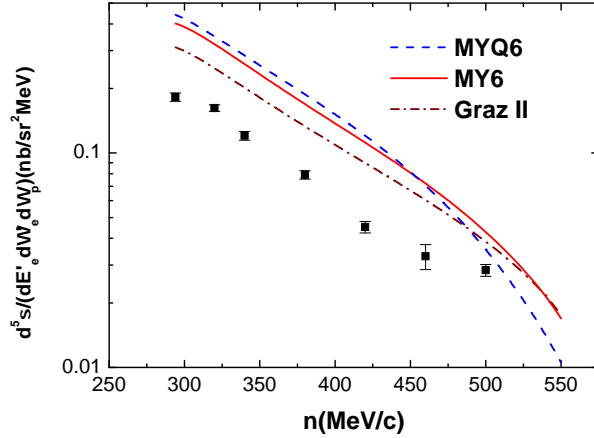


Figure 12: Cross section for the kinematical conditions [51]. See also the caption of Fig.10.

7. Acknowledgements

We wish to thank Drs. A.A. Goy, D.V. Shulga, K.Yu. Kazakov and Prof. G. Rupp for their interest in the present work and fruitful discussions. S.G.B. and V.V.B. thank the National Taiwan University for their warm hospitality.

References

- [1] G.E. Brown and A.D. Jackson, The Nucleon-Nucleon Interaction, RX-707 (NORDITA), 1974, 151pp; 1975, 387pp.
- [2] F. Gross, Relativistic Effects and Relativistic Methods, in Modern Topics in Electron Scattering, World Scientific, 1991, 219pp.
- [3] V. Pascalutsa, J.A. Tjon, Phys. Rev. C 61 (2000) 054003, nucl-th/0003050.
- [4] J.F. Mathiot, Nucl. Phys. A 412 (1984) 201.
- [5] R.F. Wagenbrunn, W. Plessas, Few Body Syst. Suppl. 8 (1995) 181.
- [6] T. Wilbois, G. Beck, H. Arenhovel, Few Body Syst. 15 (1993) 39.

- [7] J. Carbonell, B. Desplanques, V.A. Karmanov, J.F. Mathiot, Phys. Rept. 300 (1998) 215, nucl-th/9804029.
- [8] M. Gari, H. Hyuga, Z. Phys. A 277 (1976) 291.
- [9] W.Y.P. Hwang, T.W. Donnelly, Phys. Rev. C 33 (1986) 1381.
- [10] W.Y.P. Hwang, G.E. Walker, Annals Phys. 159 (1985) 118.
- [11] S.D. Kurgalin, Yu.M. Chuvilsky, Sov. J. Nucl. Phys. 49 (1989) 79.
- [12] A.Yu. Illarionov, G.I.Lykasov, Phys. Rev. C 64 (2001) 044004.
- [13] A. Faessler, V.I. Kukulín, M.A. Shikhalev, Annals Phys. 320 (2005) 71, nucl-th/0505026.
- [14] D. Chiladze *et al.* Eur. Phys. J. A 40 (2009) 23.
- [15] A.F. Krutov, V.E. Troitsky, Phys. Part. Nucl. 40 (2009) 136.
- [16] L.S. Azhgirey, N.P. Yudin, Phys. Part. Nucl. 37, No. 4 (2006) 1011.
- [17] S.G. Bondarenko, V.V. Burov, A.V. Molochkov, G.I. Smirnov, H. Toki, Prog. Part. Nucl. Phys. 48 (2002) 449, nucl-th/0203069.
- [18] M. Lacombe *et al.*, Phys. Rev. C 21 (1980) 861.
- [19] R. Machleidt, K. Holinde, Karlsruhe 1983 Proceedings, Few Body Problems In Physics, Vol. 2 (1984) 79.
- [20] L. Crepinsek, H. Oberhummer, W. Plessas, H. Zingl, Acta Phys. Austriaca 39 (1974) 345.
- [21] L. Crepinsek, C.B. Lang, H. Oberhummer, W. Plessas, H.F.K. Zingl, Acta Phys. Austriaca 42 (1975) 139.
- [22] M.I. Haftel, Phys. Rev. C 14 (1976) 698.
- [23] N. Giraud, Y. Avishai, C. Fayard, G.H. Lamot, Phys. Rev. C 19 (1979) 465.
- [24] L. Mathelitsch, W. Plessas, M. Schweiger, Phys. Rev. C 26 (1982) 65.
- [25] J. Haidenbauer, W. Plessas, Phys. Rev. C 30 (1984) 1822.

- [26] J. Haidenbauer, Y. Koike, W. Plessas, Phys. Rev. C 33 (1986) 439.
- [27] R.V. Reid, Jr., Ann. Phys. 50 (1968) 411.
- [28] D.J. Ernst, C.M. Shakin, R.M. Thaler, Phys. Rev. C 8 (1973) 46.
- [29] G. Rupp, J.A. Tjon, Phys. Rev. C 41 (1990) 472.
- [30] K. Schwarz, J. Frohlich, H.F.K. Zingl, Acta Phys. Austriaca 53 (1981) 191.
- [31] S.G. Bondarenko, V.V. Burov, K.Y. Kazakov, D.V. Shulga, Phys. Part. Nucl. Lett. 1 (2004) 178, nucl-th/0402056v2.
- [32] S.G. Bondarenko, V.V. Burov, W.-Y. Pauchy Hwang, E.P. Rogochaya, JETP Lett. 87 (2008) 653, 0804.3525v2 [nucl-th].
- [33] S.G. Bondarenko, V.V. Burov, E.P. Rogochaya, Y. Yanev, 0806.4866 [nucl-th] (2008).
- [34] S.G. Bondarenko, V.V. Burov, W.-Y. Pauchy Hwang, E.P. Rogochaya, Nucl. Phys. A 832 (2010) 233, nucl-th/0612071.
- [35] H.P. Noyes, Phys. Rev. Lett. 15 (1965) 538.
- [36] K.L. Kowalski, Phys. Rev. Lett. 15 (1965) 798.
- [37] E.E. Salpeter, H.A. Bethe, Phys. Rev. 84 (1951) 1232.
- [38] J.J. Kubis, Phys. Rev. D 6 (1972) 547.
- [39] H.A. Bethe, Phys. Rev. 76 (1949) 38.
- [40] Y. Yamaguchi, Phys. Rev. 95 (1954) 1628;
Y. Yamaguchi, Y. Yamaguchi, Phys. Rev. 95 (1954) 1635.
- [41] O. Dumbrajs *et al.*, Nucl. Phys. B 216 (1983) 277.
- [42] T.D. Lee, G.C. Wick, Nucl. Phys. B 9 (1969) 209.
- [43] N.L. Rodning, L.D. Knutson, Phys. Rev. C 41 (1990) 898.
- [44] N. Honzawa, S. Ishida, Phys. Rev. C 45 (1992) 47.

- [45] J. Fleischer, J.A. Tjon, Nucl. Phys. B 84 (1975) 375.
- [46] R. Machleidt, Phys. Rev. C 63 (2001) 024001.
- [47] R.A. Arndt, W.J. Briscoe, I.I. Strakovsky, R.L. Workman, Phys. Rev. C 76 (2007) 025209, 0706.2195v3 [nucl-th].
- [48] S.G. Bondarenko, V.V. Burov, M. Beyer, S.M. Dorkin, Phys. Rev. C 58 (1998) 3143.
- [49] S.G. Bondarenko, V.V. Burov, E.P. Rogochaya, A.A. Goy, Phys. Atom. Nucl. 70 (2007) 2054, nucl-th/0612071.
- [50] M. Bernheim *et al.*, Nucl. Phys. A 365 (1981) 349.
- [51] S. Turck-Chieze *et al.*, Phys. Lett. B 142 (1984) 145.
- [52] V.G.J. Stoks, R.A.M. Kompl, M.C.M. Rentmeester, J.J. de Swart, Phys. Rev. C 48 (1993) 792.
- [53] B. Loiseau, L. Mathelitsch, W. Plessas, K. Schwarz, Phys. Rev. C 32 (1985) 2165.